A case of hyperfunctioning pancreatic mixed adenoneuroendocrine carcinoma (MANEC) arising from ectopic pancreatic tissue in the liver

Christopher J. Steel, MD; Valerie Hostetler, MD; and Dell Dunn, MD

We report the case of a hyperfunctioning mixed adenoneuroendocrine carcinoma (MANEC) arising from ectopic pancreatic tissue in the liver. To our knowledge, the imaging appearance of a MANEC in the liver has never been reported. Literature on MANEC and its imaging features, including its appearance on the MR hepatobiliary phase and differential considerations, are reviewed and discussed.

Introduction

Pancreatic exocrine tumors make up approximately 95% of pancreatic malignancies. Those of acinar cell differentiation are the least common, making up 1-2% of exocrine pancreatic neoplasms; neuroendocrine tumors (NET) are much more common (1). There have been many reports of neuroendocrine components within pancreatic acinar cell carcinomas (ACC) with varying percentages of neuroendocrine cells and a variety of neuroendocrine cell subtypes. In 2010, the World Health Organization (WHO) defined a mixed adenoneuroendocrine carcinoma (MANEC) as a neoplasm containing at least 30% of both acinar and neuroendocrine cells (2). While approximately 40% of pancreatic ACC contain neuroendocrine cells, fewer than 30 cases of MANEC with pancreatic acinar differentiation have been reported in the literature (3). Malignant transformation within ectopic pancreatic tissue is also exceedingly rare, with fewer than 15 cases reported in the literature (4).

The authors are all in the Department of Radiology at the David Grant USAF Medical Center, Travis AFB, CA. Contact Dr. Steel at Christopher.Steel.1@us.af.mil.

Case report

A 65-year-old male with a past medical history of peptic ulcer disease presented to the emergency department with complaints of nausea, vomiting, frequent watery melanotic stools, tremors, and right-upper-quadrant abdominal pain of approximately 1 week's duration. Pertinent negatives included no history of liver dysfunction, malignancy, diabetes, arthralgias, or skin rashes.

The patient had stable vital signs and was in no acute distress. There were hyperactive bowel sounds, and the patient's epigastrium was tender to palpation without rebound tenderness or peritoneal signs.

The patient had a normal WBC of 9.5 x109/L (normal range: 4.4- 11.3 x109/L) as well as lipase of 19 U/L (normal range: 13 − 60 U/L). Outside of a slight elevation of LDH to 230 (normal range: 135 - 225 U/L), the patient's hepatic panel was unremarkable, with albumin 3.8 g/dL (normal range: 3.5 − 5.2 g/dL), AST 26 U/L (normal range: 0 − 40 U/L), ALT 14 U/L (normal range: 0 − 41 U/L), alkaline phosphatase 118 (normal range: 40 − 129 U/L), and total bilirubin 0.7 mg/dL (normal range: 0.1 − 1.2 mg/dL).

Abdominal radiographs demonstrated a mass in the upper abdomen with mass effect on the surrounding bowel (Fig. 1). A subsequent CT of the abdomen and pelvis, enhanced with intravenous and oral contrast and imaged during the portal venous phase, revealed a lobulated 13.5 x 11.8 x 10.5-cm, heterogeneously enhancing mass in the left hepatic lobe, with central hypoattenuating material thought to represent necrosis (Fig. 2). There was no imaging evidence of cirrhosis or portal hypertension. Outside of a 7mm hypodensity in the pancreatic head, the pancreas was unremarkable, with no suspicious mass (Fig. 3).

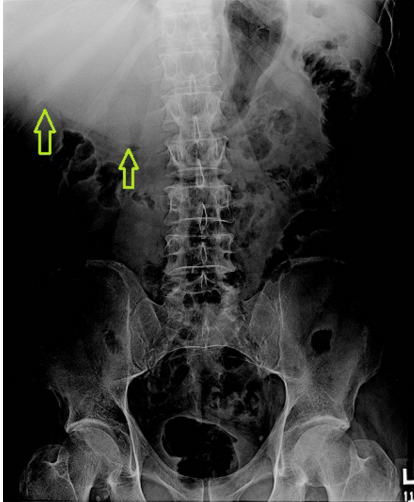# Hyperfunctioning MANEC arising from ectopic pancreatic tissue in the liver

Figure 1. 65-year-old male with pancreatic differentiated MANEC within the left hepatic lobe. Frontal radiograph of the abdomen demonstrates a large opacity (open arrows) in the right upper quadrant with mass effect on the adjacent air-filled bowel and stomach.
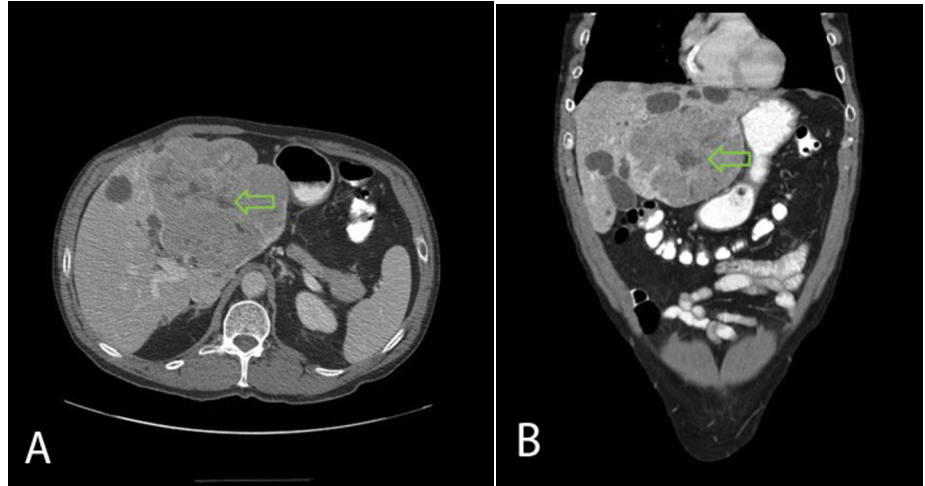

Figure 2. 65-year-old male with pancreatic differentiated MANEC within the left hepatic lobe. Axial (A) and coronal (B) CT images of the abdomen show a 13.5 x 11.8 x 10.5-cm, heterogeneously enhancing mass in the left hepatic lobe with central hypodensity (open arrow). No calcifications or satellite lesions are seen. Incidental simple hepatic cysts are nearby.
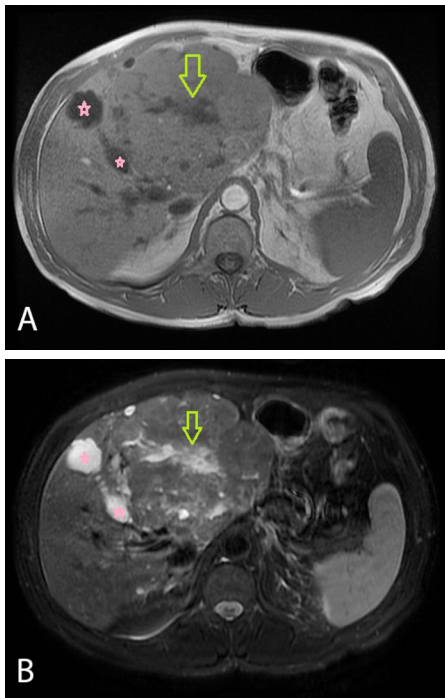

Figure 3. 65-year-old male with pancreatic differentiated MANEC within the left hepatic lobe. Axial T1 (A) and T2 (B) weighted images show a large lobulated tumor in the left hepatic lobe with a T1- hypointense, T2-hyperintense scar (open arrow) with multiple surrounding simple cysts (stars) and intratumoral foci of hemorrhage at the periphery.
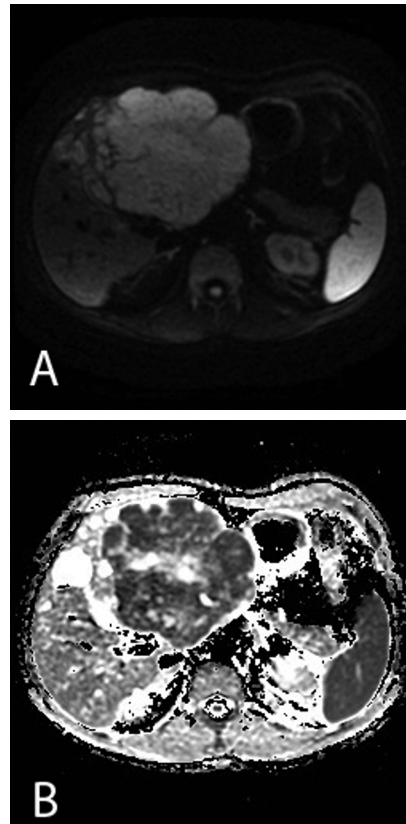

Figure 4. 65-year-old male with pancreatic differentiated MANEC within the left hepatic lobe. Axial diffusion-weighted imaging (A) demonstrates high signal throughout the tumor. The corresponding ADC sequence (B) shows high signal intensity within the central scar due to T2 "shine-through" and confirms restricted diffusion in the surrounding tumor parenchyma.

Additional laboratory workup after admission included a hepatitis panel that showed a positive hepatitis B virus core antibody (HBcAb). The patient's serum alpha-fetoprotein level (AFP) was within normal limits at 2.55 ng/mL (normal range: 0-8.30 ng/mL).
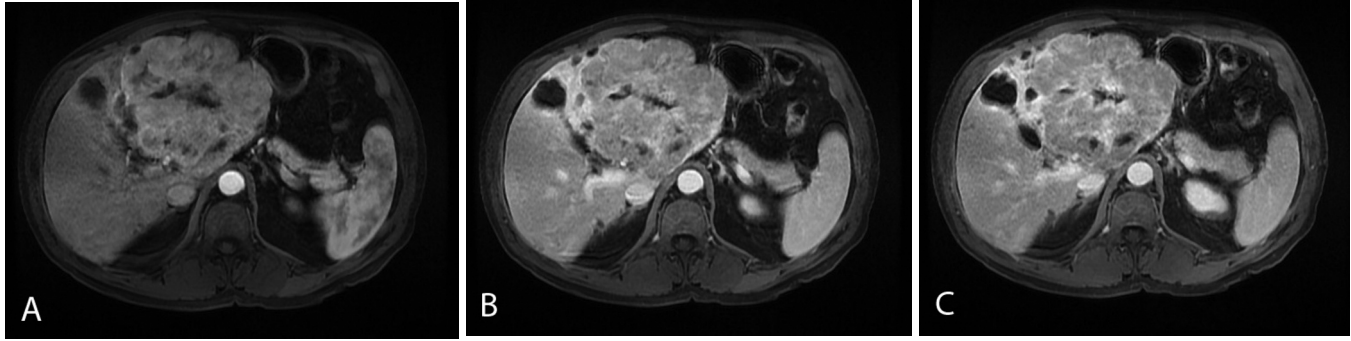
Figure 5. 65-year-old male with pancreatic differentiated MANEC within the left hepatic lobe. Contrast-enhanced axial LAVA FS images during the arterial phase (A), at 5 min (B), and at 10 min (C) demonstrate arterial enhancement of the MANEC followed by slight washout relative to the liver. The central scar demonstrates delayed enhancement (C).
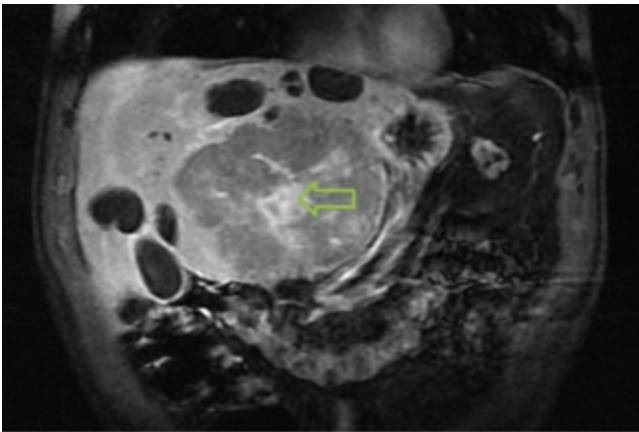

Figure 6. 65-year-old male with pancreatic differentiated MANEC within the left hepatic lobe. Contrast-enhanced coronal LAVA FS image at 60 minutes (hepatobiliary phase) demonstrates no retention of the hepatobiliary agent in the tumor parenchyma. Progressive enhancement of the central scar is seen, but not due to biliary excretion of the hepatobiliary agent; rather, the dense cellular matrix of the scar traps the gadolinium chelate.

Further evaluation with a gadolinium-enhanced MRI of the abdomen, using the hepatocyte-specific contrast agent gadobenate dimeglumine, demonstrated an isointense mass on T1 and T2 sequences, with a T2-hyperintense central scar (Fig. 4). The tumor was heterogeneously hyperenhancing in the arterial phase, with relative washout in the portal venous phase. A central scar was noted that demonstrated progressive accumulation of the gadolinium-based contrast agent (GBCA) on 10-minute delayed and hepatobiliary (60-minute) phases (Figs. 5, 6).

No solid mass was seen in the pancreas on MRI. The 7mm pancreatic head hypodense lesion was shown to be cystic without internal septation, or nodularity. While lesions this small are difficult to characterize, statistically this would most likely represent a benign intrapancreatic mucinous neoplasm and is unrelated to the liver mass. 18

months of subsequent followup has not shown any change in this cystic lesion.

There were multiple simple cysts, with no other suspicious liver lesions identified. There were no signs of cirrhosis and no evidence of metastatic spread to lymph nodes or other organs.

Based on the MRI findings, a biopsy of the liver mass was recommended for further evaluation. Ultrasound-guided biopsy of the liver produced initial pathology results consistent with a low-grade (well differentiated) neuroendocrine tumor (NET) with negative hepatic markers.

A 24-hour urine specimen showed normal 5-Hydroxyindoleacetate (5-HIAA) of 3.9 mg/24 hrs. (normal: 6.0 mg/24 hrs. or less). The surgical oncologist requested an indium-111 pentreotide (Octreoscan) test be-

Figure 7. 65-year-old male with pancreatic differentiated MANEC within the left hepatic lobe. Whole-body planar images 24 hours after the administration of 5.98 mCi of indium-111 demonstrate physiologic uptake within the liver, spleen, kidneys, and bowel with no evidence of radiotracer uptake within the hepatic tumor.
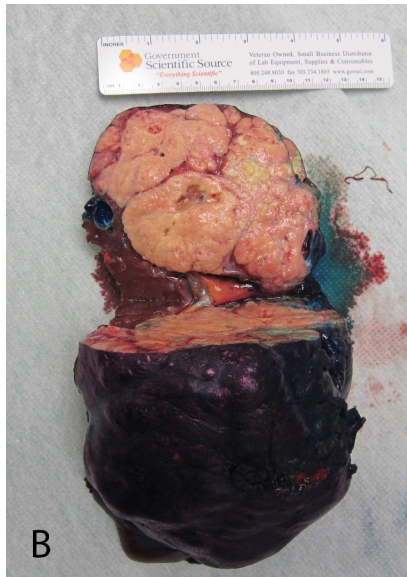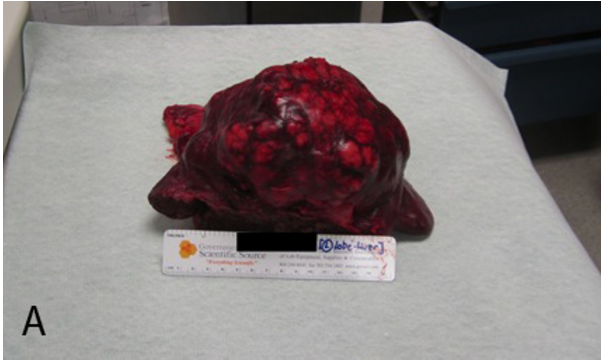
Figure 8. 65-year-old male with pancreatic differentiated MANEC within the left hepatic lobe. (A) The large lobulated tumor within the left hepatic lobe, status post lobectomy. (B) The transected tumor with a central stellate scar.

larger size, other symptoms can include nausea, vomiting, weight loss, and jaundice. While MANECs contain neuroendocrine cells, the vast majority of these tumors are non-hyperfunctioning or nonsyndromic, suggesting that these cells remain in a primitive state or produce immature hormones (1). That being said, there are case reports of hyperfunctioning MANECs presenting with symptoms of watery diarrhea, similar to this case, as well as Zollinger-Ellison Syndrome (6, 7). A subset of pure ACC develops a lipase hypersecretion syndrome characterized by skin rashes, arthralgias, and fat necrosis.
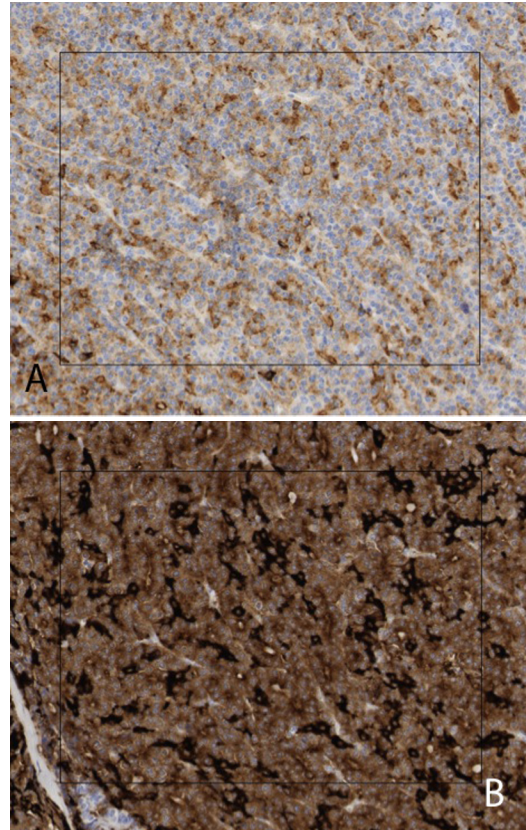
Figure 9. 65-year-old male with pancreatic differentiated MANEC within the left hepatic lobe. Immunohistochemical stains of the MANEC demonstrate weak, diffuse staining with chromogranin (A) and patchy staining with synaptophysin (B), both of which are neuroendocrine markers. The WHO requirement for the diagnosis of MANEC requires at least 30% acinar and neuroendocrine differentiation.

cause the origin of the neuroendocrine tumor was not clear, based on imaging and biopsy. This study revealed no tracer uptake in the hepatic mass, pancreas, bowel, or elsewhere in the body (Fig. 7). The patient proceeded to left hepatic lobectomy, with specimens sent to two separate tertiary referral centers for consultation (see Fig. 8 for gross specimen). Additional immunohistochemical stains demonstrated a moderately poorly differentiated carcinoma with mixed neuroendocrine and acinar cell differentiation, with stronger chromogranin consistent with predominant neuroendocrine differentiation (Fig. 9). The final pathology diagnosis was MANEC, with the report suggesting that the most likely source as metastasis from the pancreas or (less likely) ectopic pancreatic tissue in the liver. However, followup imaging over 14 months has demonstrated no evidence of recurrent disease, nor has a primary pancreatic mass manifested itself, leading us to conclude that the tumor did indeed arise from ectopic pancreatic tissue in the liver.

Discussion

Patients with MANEC of the pancreas tend to be middle-aged and present with nonspecific symptoms, commonly vague abdominal pain (5). Due to the propensity of this tumor to arise in the pancreatic head, as well as its

Reported MANECs in the pancreas have been large (>7cm), and are most commonly found in the pancreatic head. Additionally, as demonstrated in this case, a MANEC can arise in other organs with no evidence of pancreatic involvement. Review of the literature illustrated 5 cases arising from the stomach (8-10). It is theorized that pancreatic metaplasia or ectopic pancreatic tissue may account for these extrapancreatic MANECs. Metastatic disease has

Condition	Seen on CT	Seen on MRI
Fibrolamellar HCC	* Large, well circumscribed mass with hypodense central scar (70%) * Heterogeneously arterial enhancement * Scar may show late enhancement (10-15 min)	* Heterogeneous arterial enhancement of the mass
FNH	* Hypodense to isodense mass * 50% contain a central scar * Homogeneous arterial enhancement that fades away, becomine isodense to normal liver * Scar demonstrates delayed enhancement (3-5 min)	* Iso- to hypo-isointense on T1, mildly hyper-isointense on T2, with T2 bright central scar * Arterial phase homogeneous enhancement of the tumor with lack of scar enhancement. Tumor gradually decreases to liver intensity while the scar enhances in delayed/hepatobiliary phases. * Hepatobiliary phase rentention of contrast is nearly diagnostic
HCC	* NECT: Hypodense mass, may develop central necrosis * Arterial enhancement with portal venous washout * Larger masses may have necrotic areas or vascular invasion	* Variable T1 signal, T2 iso- to hyperintense * Arterial enhancement with delayed washout
Cavernous hemangioma	* Hypodense mass, may appear heterogenseous with central scar when large * Peripheral nodular enhancement with progressive centripetal fill-in	* Hypointense on T1, hyperintense on T1 * Hepatocyte-specific contrast agent will mirror the blood vessels, and at time show "pseudo-washout" in the equilibrium phase due to rapid uptake by the liver
Hepatic metastases	* Multifocal * Central scar has been reported on some larger metastases, but necrosis is much more common	* High T2 signal intensity
MANEC	* Large, heterogeneously enhancing mass with central necrosis * Look for pancreatic primary mass	* Isointense on T1 and T2 * T2-hyperintense central scar * Early arterial enhancement and washout in the portal venous phase with retention in the central scar

Table. Differential diagnosis for a hepatic tumor with a central scar

been reported both in tumors arising from the pancreas as well from in those originating in other organs.

To our knowledge, only one paper has been dedicated to describing the imaging findings of a MANEC (11). In that case, CT demonstrated a heterogeneous, hypoattenuating, 8 x 2.5-cm mass within the pancreatic tail with capsule-like enhancement. On MRI, the mass was T2-heterogeneously hyperintense with a T2-hypointense nodular focus. The tumor demonstrated heterogenous enhancement, with more diffuse enhancement in the previously described nodule. Given the limited number of cases in the literature, there are no classic imaging findings for this particular tumor, and previous studies have combined MANEC with pure ACC in analyses.

With such little information available, it is worthwhile to describe the appearance of pancreatic ACC, as the acinar component may result in similar imaging features. These tumors are often found in the pancreatic head and tend to be large at presentation with a mean diameter of 7.1 cm (12). Presenting symptoms may include arthralgias, skin rashes, and fat necrosis from lipase hypersecretion. Larger ACCs tend to develop cystic areas centrally, likely related to

necrosis. The most common enhancement pattern reported tends to be hypovascular relative to the pancreas and homogeneous. ACC in the pancreas has not been described with a central scar. Calcification is reported in a small minority of pancreatic ACCs (6%). Hepatic metastases from ACC tend to be lobulated and well defined, and enhance less than hepatic parenchyma.

Given the rarity of this diagnosis, one of the greatest utilities of discussing this case is generating a differential for this mass and highlighting why it does not fit the classic pattern for more prevalent diagnoses. One of the more notable findings to base a differential on was the central scar within the mass. The classic differential for a hepatic mass with a central scar includes, among many others (Table), fibrolamellar HCC and focal nodular hyperplasia (FNH). Fibrolamellar HCC is ordinarily seen in young adults with noncirrhotic livers. These masses present as large, well-circumscribed hepatic tumors with a hypodense central scar. Unlike the case presented, the true central scar of fibrolamellar HCC appears hypointense on both T1 and T2 sequences; only a small subset demonstrate delayed enhancement of the scar. This is in contradistinction to FNH, in which the central "scar" is actually an aggregate of vessels and bile ducts (13). On NECT, an FNH scar appears hypoattenuating to isodense to liver. On MRI, it is generally hypointense to isointense on T1, and slightly hyperintense on T2 with a bright central scar, similar to the MANEC presented here (14). Multiphase MRI evaluation shows homogeneous arterial enhancement of a well-defined, lobulated tumor with initial hypointensity of the central scar. On delayed phases, the tumor will fade in signal intensity to approach that of the background liver, while the central "scar" will gradually enhance until hyperintense delayed phases. The retention of contrast in the tumor parenchyma in FNH distinguishes it from tumors without functional hepatocytes and from the MANEC, which did not retain the hepatobiliary agent in the tumor parenchyma during the hepatobiliary phase.

The behavior of the central scar in this case was interesting and represented a potential pitfall on the 60-minute delayed hepatobiliary phase. Though exceptions exist, retention of hepatobiliary specific contrast agents in tumor parenchyma at hepatobiliary phase suggests functioning hepatocytes (15). However, this lesion had no retention in the tumor parenchyma. The accumulation in scars is a typical feature of all GBCA, and this trapping of contrast is an essential tool in cardiac MRI, resulting from a reduced ability of the scar tissue to clear the gadolinium deposited there.

At initial presentation, hepatocellular carcinoma (HCC) was a legitimate concern in the setting of a single hepatic lesion and no other suspicious abdominal masses. With no indicators of active infection, the patient's positive hepatitis B core antibody was likely an indicator of resolved infection or a false positive test. While there are cases of HCC documented in patients with noncirrhotic livers and HBcAb and surface antibodies, in general the hepatitis B replication rate is low or absent in the setting of isolated

HBcAb, and the risk of HCC is low (16, 17). In noncirrhotic livers, HCC can present as large masses with central necrosis. On contrast-enhanced CT (CECT), they usually enhance heterogeneously in the arterial phase, with washout in the portal venous phase. MRI features include variable T1 signal, mild T2 hyperintensity, and heterogenous arterial phase enhancement, with subsequent washout in the remaining phases. These characteristic findings are not consistent with the MANEC reported, which was isointense on T1 and T2, diffusely enhancing, and exhibited delayed scar enhancement. There are cases where moderate- to well-differentiated HCCs can retain some capacity in handling bile and infrequently retain gadobenate dimeglumine in the parenchyma during the hepatobiliary phase (18).

Cavernous hemangiomas are the most common benign primary hepatic tumors. Given the large size of the case reported, a giant cavernous hemangioma might have been a consideration. On NECT, they appear heterogeneous and (when large) can occasionally contain a central hypoattenuating scar. However, CECT would show peripheral nodular enhancement in the arterial phase, with progressive centripetal enhancement in the venous and delayed phases. Cavernous hemangiomas are hypointense on T1 and markedly hyperintense on T2. If a central scar is present, it will not demonstrate enhancement (20). Extracellular contrast agents usually demonstrate similar features to CECT, while hepatocyte-specific contrast agents will mirror the blood vessels and at times show "pseudo washout" in the equilibrium phase due to rapid uptake by the liver (19).

Early pathologic reports from the biopsy of the MANEC suggested a well-differentiated NET. The negative hepatic markers were not consistent with a primary hepatic NET (also known as primary hepatic carcinoid), another very rare tumor. Primary hepatic NETs appear variable on T2 and hypointense on T1, and demonstrate heterogeneous enhancement in the arterial phase with washout in the portal venous phase. There are reports of contrast accumulation in central scars of hepatic NETs during the equilibrium phase; however, no data was found on the hepatobiliary phase (20). Liver metastases are commonly seen with pancreatic or small-bowel NETs. On MRI, these lesions are hypointense on T1 and hyperintense on T2. They are known for being hypervascular and demonstrate early, intense, homogeneous enhancement or occasionally peripheral rim enhancement, with progressive fill-in on delayed images (21). The lack of In-111 on the Octreoscan, while not definitive alone, provided molecular imaging evidence against a NET diagnosis.

To summarize the comparison to these primary hepatic tumors, the presence of a scar and a noncirrhotic liver made HCC very unlikely. While the overall appearance was most similar to FLHCC, the T2 hyperintensity of the scar and patient age did not fit. The size, foci of necrosis, and lack of functional hepatocytes as shown on the hepatobiliary phase excluded FNH. The enhancement pattern of this mass did not parallel the blood pool to support a cavernous hemangioma, and the central scar in a heman-

gioma would not enhance. A primary hepatic NET is another rare consideration; however, imaging findings to include nuclear medicine studies did demonstrate classic features.

Surgery is the treatment of choice if a MANEC is resectable; however, there is no large-scale followup data for alternatives such as tumor debulking or antiproliferative therapy. A review examined the first eleven pancreatic MANECs and found that four patients died from 5 to 24 months after diagnosis, while six were disease-free 4 to 72 months after the initial diagnosis (21). In this case, followup imaging has demonstrated no evidence of recurrent or residual disease for over 18 months.

Conclusion

Pancreatic MANEC is a rare neoplasm that can be discovered as an isolated finding in organs other than the pancreas, with radiological features that can mimic more common tumors. Multiphase MRI can help further narrow the differential and exclude other more prevalent tumors.

References

1. Lee L, Bajor-Dattilo EB, Das K. Metastatic mixed acinar-neuroendocrine carcinoma of the pancreas to the liver: a cytopathology case report with review of the literature. *Diagnostic Cytopathology*. 2012; 41(2):164–170. [PubMed]
2. Bosman F, Carneiro F, Hruban R, Theise N, eds. *WHO classification of tumours of the digestive system*. Lyon, France: IARC Press; 2010: 418p.
3. Stelow EB, Shaco-levy R, Bao F, Garcia J, Klimstra DS. Pancreatic acinar cell carcinomas with prominent ductal differentiation: Mixed acinar ductal carcinoma and mixed acinar endocrine ductal carcinoma. *Am J Surg Pathol*. 2010; 34(4):510-8. [PubMed]
4. Okamoto H, Kawaoi A, Ogawara T, Fujii H. Invasive ductal carcinoma arising from an ectopic pancreas in the gastric wall: a long-term survival case. *Case Rep Oncol*. 2012; 5(1):69-73. [PubMed]
5. Shi C, Jin D, Lou W. Mixed acinar-endocrine carcinomas of the pancreas: case report and literature review. *Surgical Practise*. 2008; 12(3):89–92. [PubMed]
6. Ordóñez NG, Balsaver AM, Mackay B. Mucinous islet cell (amphicrine) carcinoma of the pancreas associated with watery diarrhea and hypokalemia syndrome. *Hum Pathol*. 1988; 19(12):1458-61. [PubMed]
7. Terada T, Matsunaga Y, Maeta H, Endo K, Horie S, Ohta T. Mixed ductal-endocrine carcinoma of the pancreas presenting as gastrinoma with Zollinger-Ellison syndrome: an autopsy case with a 24-year survival period. *Virchows Arch*. 1999; 435(6):606-11. [PubMed]
8. Kusafuka, K, Bando E, Muramatsu K, et al. Pancreatic-type mixed acinar-endocrine carcinoma with alpha-fetoprotein production arising from the stomach: A report of an extremely rare case. *Medical Molecular Morphology*. 2009; 42(3):167-74. [PubMed]
9. Fukunaga M. Gastric carcinoma resembling pancreatic mixed acinar-endocrine carcinoma. *Hum Pathol*. 2002; 33(5):569-73. [PubMed]
10. Jain D, Eslami-Varzaneh F, Takano AM, Ayer U, Umashankar R, Muller R, Klimstra DS. Composite glandular and endocrine tumors of the stomach with pancreatic acinar differentiation. *Am J Surg Pathol*. 2005; 29(11):1524-9. [PubMed]
11. Chung WJ, Byun JH, Lee SS, Lee MG. Imaging findings in a case of mixed acinar-endocrine carcinoma of the pancreas. *Korean J Radiol*. 2010 May-Jun; 11(3):378-81. [PubMed]
12. Tatli S, Mortele KJ, Levy AD, Glickman JN, Ros PR, Banks PA, Silverman SG. CT and MRI features of pure acinar cell carcinoma of the pancreas in adults. *AJR Am J Roentgenol*. 2005 Feb; 184(2):511-9. [PubMed]
13. Campos JT, Sirlin CB, Choi JY. Focal hepatic lesions in Gd-GD-EOB-DTPA enhanced MRI: the atlas. *Insights Imaging*. 2012 Oct; 3(5):451–474. [PubMed]
14. Hussain SM, Terkivatan T, Zondervan PE, Lanjouw E, de Rave S, Ijzermans JN, de Man RA. Focal nodular hyperplasia: findings at state-of-the-art MR imaging, US, CT, and pathologic analysis. *Radiographics*. 2004 Jan-Feb; 24(1):3-17. [PubMed]
15. Van Beers BE, Pastor CM, Hussain HK. Primovist, Eovist: what to expect. *Journal of Hepatology*. 2012 Aug; 57:421–429. [PubMed]
16. Seattle STD/HIV Prevention Training Center and the University of Washington. "Discussion - Interpretation of Isolated Hepatitis B Core Antibody - Hep B - Hepatitis Web Study." *Hepatitis Web Study*, 2013. Web. 14 Aug. 2014
17. Kalayci C, Johnson PJ, Davies SE, Williams R. Hepatitis B virus related hepatocellular carcinoma in the non-cirrhotic liver. *J Hepatol*. 1991 Jan;12(1):54-9. [PubMed]
18. Kim SH, Kim SH, Lee J, Kim MJ, Jeon YH, Park Y, Choi D, Lee WJ, Lim HK. Gadoxetic acid-enhanced MRI versus triple-phase MDCT for the preoperative detection of hepatocellular carcinoma. *Am J Roentgenol*. 2009 Jun; 192(6):1675-81. [PubMed]
19. Kim YC, Park MS, Chung YE, Kim MJ, Park YN, Kang JH, Kim KA, Kim KW. MRI findings of uncommon non-hepatocyte origin primary liver tumours with pathological correlation. *Br J Radiol*. 2010 Dec; 83(996):1080-6. [PubMed]
20. Bader TR, Semelka RC, Chiu VC, Armao DM, Woosley JT. MRI of carcinoid tumors: spectrum of appearances in the gastrointestinal tract and liver. *J Magn Reson Imaging*. 2001 Sep; 14(3):261-9. [PubMed]
21. Ballas KD, Rafailidis SF, Demertzidis C, Alatsakis MB, Pantzaki A, Sakadamis AK. Mixed exocrine-endocrine tumor of the pancreas. *JOP*. 2005 Sep 10; 6(5):449-54. [PubMed]